Ray-tracing simulations and applications of liquid crystal beam control devices

Maarten Sluijter[a], Dick K.G. de Boer[a], H. Paul Urbach[b], Jan Strömer[a] and Giovanni Cennini[a]

[a]Philips Research Europe, High Tech Campus 34, Eindhoven, The Netherlands;
[b]Optics Research Group, Department Imaging Science and Technology,
Delft University of Technology, Lorentzweg 1, Delft, The Netherlands

ABSTRACT

We have developed a general ray-tracing method in the geometrical-optics approach which enables the modeling of in general inhomogeneous liquid crystal configurations. In this manuscript, we discuss two prominent examples in which we calculate the optical properties of two liquid crystal configurations. We first present simulations of a liquid crystal-based electro-optical device that enables a switching effect due to a back reflection phenomenon. In these simulations, we exploit the optical properties of a liquid crystal with a special Freédericksz alignment. Secondly we present preliminary results of the optical properties of a liquid crystal-based optical element that can actively control guiding and extraction of light. A promising application of such a device can be found in for example beam control devices for lighting applications or applications that require local dimming and highlighting.

Keywords: Liquid crystal, geometrical optics, ray tracing, inhomogeneous media, birefringent media

1. INTRODUCTION

We have developed a ray-tracing method in the geometrical-optics approach that is based on the Hamiltonian principle.[1] This method is called the Hamiltonian method and enables the calculation of the optical properties of uniaxially anisotropic media. In particular, the method incorporates the fact that inside inhomogeneous anisotropic media, ray paths of light rays are curved. The Hamiltonian method is based upon one important assumption: the properties of an inhomogeneous anisotropic medium are assumed to change slowly over the distance of a wavelength. In the way we presented the theory, the ray-tracing formulas are ready for use and easy to implement in a ray-tracing simulation program. We will show that the use of the Hamiltonian method in a ray-tracing simulation program facilitates the modeling of inhomogeneous anisotropic media. In this manuscript, we focus our attention to inhomogeneous liquid crystal configurations and discuss two prominent examples.

First we will present simulations of a liquid crystal-based electro-optical device that enables a switching effect due to a back reflection phenomenon.[2] In the simulations, we exploit the optical properties of a liquid crystal with a special Freédericksz alignment. We will show that a two-dimensional gradient in a liquid crystal layer applied between two parallel mirrors enables a back reflection phenomenon in which the direction of propagation of extraordinary light rays is reversed. Possible applications of the liquid crystal device can be found in, but are not restricted to, optical communication systems and lighting applications.

Secondly we discuss some preliminary ray-tracing results of the optical properties of a liquid crystal-based optical element[3] that can actively control guiding and extraction of light. A promising application of such a device can be found in for example beam control devices for lighting applications or applications requiring local dimming and highlighting. Light that is extracted from the optical element is linearly polarized, a feature that is desired for applications such as backlight architectures for liquid crystal displays (LCDs). In contrast with direct-lit geometries, the optical element is suitable for side-lit configurations. The advantage of this technology is that it offers a reduction in power consumption, since it is capable of local dimming and highlighting with a low number of light sources. Different types of side-lit configurations that produce light with a specific polarization

Further author information: (Send correspondence to M. Sluijter)
M. Sluijter: E-mail: Maarten.Sluijter@philips.com, Telephone: +31 40 2747569

Emerging Liquid Crystal Technologies IV, edited by Liang-Chy Chien, Ming Hsien Wu,
Proc. of SPIE Vol. 7232, 72320S · © 2009 SPIE · CCC code: 0277-786X/09/$18 · doi: 10.1117/12.816508

have been investigated in the past. One approach consists of a system using birefringent material applied on a micro-structured light guide.[4,5] However, the optical element discussed in this manuscript forms a basis for a novel approach to enable a side-lit geometry.[3] This approach does not require the manufacturing of microstructures. It enables a controlled guiding and extraction of polarized light and a high resolution that is independent of the number of light sources.

2. HAMILTONIAN METHOD FOR INHOMOGENEOUS ANISOTROPIC MEDIA

For the calculation of the ray path of a light ray inside an inhomogeneous medium, we can apply the Hamiltonian principle. The Hamiltonian principle, introduced by Kline and Kay,[6] can be considered the fundamental basis for the ray-tracing process in inhomogeneous media. However, the Hamiltonian principle does not immediately provide a set of ray-tracing equations in which the position-dependent material properties of an anisotropic medium are explicitly included. In previous work, building further on the Hamiltonian principle, we have introduced general ray-tracing equations that explicitly depend on the position-dependent material properties of uniaxially anisotropic media.[1] The general ray-tracing equations based on the Hamiltonian principle are called the Hamilton equations. In the way we presented the theory, the Hamilton equations are ready for use and easy to implement in a ray-tracing simulation program. In other work, we have extended the general ray-tracing method for inhomogeneous biaxially anisotropic media.[7] The derivation of the Hamilton equations for biaxial anisotropy involves a more complicated process than for uniaxial anisotropy. However, in this manuscript, we focus our attention to uniaxially anisotropic media only.

When polarized ray tracing is applied to an optical system, we are mainly interested in the energy flux, represented by the Poynting vector. In anisotropic media, the Poynting vector and wave vector are not parallel in general, since the electric field vector $\mathbf{E}$ and the electric flux density vector $\mathbf{D}$ are not parallel. For this reason, we define a ray as the trajectory of the Poynting vector rather than the orthogonal trajectory of the wave front (i.e. the trajectory of the wave vector).

With $\mathbf{r}$ the position of a ray and $\mathbf{p}$ a vector with the direction of the local phase velocity and length equal to the refractive index, the Hamilton equations are given by

$$\frac{d\mathbf{r}(\tau)}{d\tau} = \sigma\nabla_p\mathcal{H}(\hat{\mathbf{d}}), \tag{1}$$

$$\frac{d\mathbf{p}(\tau)}{d\tau} = -\sigma\nabla_r\mathcal{H}(\hat{\mathbf{d}}), \tag{2}$$

where τ is a parameter which can be considered as time and the factor σ is an arbitrary function of τ. In addition, the gradients $\nabla_r\mathcal{H}$ and $\nabla_p\mathcal{H}$ are functions of the local optical axis $\hat{\mathbf{d}}(\mathbf{r})$ (the director), the momentum $\mathbf{p}(\mathbf{r})$ and the ordinary and extraordinary index of refraction of the anisotropic medium, n_o and n_e respectively. In general, the refractive indices n_o and n_e can also depend on position. The scalar function $\mathcal{H}$ is called the optical indicatrix and defines the anisotropy of the vector $\mathbf{p}$. Moreover, $\nabla_p\mathcal{H}$ is a vector parallel to the Poynting vector. For uniaxially anisotropic media, we have derived the position-dependent optical indicatrix given by[1]

$$\mathcal{H}(\mathbf{r},\mathbf{p}) = \left[n_o^2|\mathbf{p}|^2 + (n_e^2 - n_o^2)(\mathbf{p}\cdot\hat{\mathbf{d}})^2 - n_o^2 n_e^2\right]\left(|\mathbf{p}|^2 - n_o^2\right) = 0. \tag{3}$$

Apparently, $\mathcal{H} = \mathcal{H}_e\mathcal{H}_o$, where $\mathcal{H}_e$ represents the optical indicatrix for extraordinary rays and $\mathcal{H}_o$ represents the optical indicatrix for ordinary rays. Then the gradient of $\mathcal{H}(\mathbf{r},\mathbf{p})$ can in general be written as

$$\nabla\mathcal{H} = \nabla\left(\mathcal{H}_e\mathcal{H}_o\right) = \mathcal{H}_e\nabla\mathcal{H}_o + \mathcal{H}_o\nabla\mathcal{H}_e. \tag{4}$$

For extraordinary rays, $\mathcal{H}_e = 0$ and then Eq. 4 reduces to

$$\nabla\mathcal{H} = \mathcal{H}_o\nabla\mathcal{H}_e. \tag{5}$$

When we substitute Eq. 5 into the Hamilton equations, the factor $\mathcal{H}_o$ can be incorporated in the parameter σ. Then we find the Hamilton equations for extraordinary rays:

$$\begin{aligned} \frac{d\mathbf{r}}{d\tau} &= \sigma \nabla_p \mathcal{H}_e(\mathbf{r}, \mathbf{p}_e), && (6) \\ \frac{d\mathbf{p}_e}{d\tau} &= -\sigma \nabla_r \mathcal{H}_e(\mathbf{r}, \mathbf{p}_e). && (7) \end{aligned}$$

With the help of Eq. 3, we calculate the gradients of the extraordinary Hamiltonian $\mathcal{H}_e(\mathbf{r}, \mathbf{p}_e)$ with respect to position and momentum and then we find

$$\begin{aligned} \frac{\partial \mathcal{H}_e}{\partial i} &= 2(n_e^2 - n_o^2)(\mathbf{p}_e \cdot \hat{\mathbf{d}}) \left(\mathbf{p}_e \cdot \frac{\partial \hat{\mathbf{d}}}{\partial i} \right) + \\ & \quad \left[(\mathbf{p}_e \cdot \hat{\mathbf{d}})^2 - n_o^2 \right] \frac{\partial n_e^2}{\partial i} + \left[|\mathbf{p}_e|^2 - (\mathbf{p}_e \cdot \hat{\mathbf{d}})^2 - n_e^2 \right] \frac{\partial n_o^2}{\partial i}, && (8) \\ \frac{\partial \mathcal{H}_e}{\partial p_{ei}} &= 2n_o^2 p_{ei} + 2(n_e^2 - n_o^2)(\mathbf{p}_e \cdot \hat{\mathbf{d}}) \hat{d}_i, \quad i = x, y, z. && (9) \end{aligned}$$

For ordinary rays $\mathcal{H}_o = 0$ and then the Hamilton equations can be written as

$$\begin{aligned} \frac{d\mathbf{r}}{d\tau} &= \sigma \nabla_p \mathcal{H}_o(\mathbf{r}, \mathbf{p}_o), && (10) \\ \frac{d\mathbf{p}_o}{d\tau} &= -\sigma \nabla_r \mathcal{H}_o(\mathbf{r}, \mathbf{p}_o), && (11) \end{aligned}$$

where the factor $\mathcal{H}_e$ is incorporated into the parameter σ. In this case, the gradients $\nabla_r \mathcal{H}_o(\mathbf{r}, \mathbf{p}_o)$ and $\nabla_p \mathcal{H}_o(\mathbf{r}, \mathbf{p}_o)$ are defined

$$\begin{aligned} \frac{\partial \mathcal{H}_o}{\partial i} &= -\frac{\partial n_o^2}{\partial i}, && (12) \\ \frac{\partial \mathcal{H}_o}{\partial p_{oi}} &= 2p_{oi}, \quad i = x, y, z. && (13) \end{aligned}$$

As a result, the Hamilton equations for ordinary rays are given by

$$\begin{aligned} \frac{d\mathbf{r}}{d\tau} &= 2\sigma \mathbf{p}_o, && (14) \\ \frac{d\mathbf{p}_o}{d\tau} &= \sigma \nabla_r n_o^2. && (15) \end{aligned}$$

For the remainder of this manuscript, we assume that the indices n_o and n_e do not depend on the position $\mathbf{r}$ but only the direction of the optical axis changes with position, as is the case in a liquid crystal. Then, for ordinary light rays, the vector $\mathbf{p}_o(\tau)$ is constant and the ray path $\mathbf{r}(\tau)$ is represented by a straight line. For extraordinary light rays, the ray path is curved in general.

The Hamilton equations for ordinary and extraordinary rays are a set of six coupled first-order differential equations for the vector components of the position $\mathbf{r}(\tau)$ and momentum $\mathbf{p}(\tau)$. Let $\mathbf{r}(\tau_0)$ and $\mathbf{p}(\tau_0)$ be the initial values for the position and momentum. Then, by taking steps $\Delta\tau$, the ray path $\mathbf{r}(\tau_0 + N\Delta\tau)$ and the corresponding momentum $\mathbf{p}(\tau_0 + N\Delta\tau)$, with $N \in \mathbb{N}$, can be calculated by using the Runge-Kutta method.[8]

The general ray-tracing equations presented in the previous analysis are ready for use and easy to implement in a ray-tracing simulation program. To prove this, we have implemented the vector equations in a ray-tracing program. This ray-tracing program can be applied to complex liquid crystal configurations with inhomogeneous anisotropic properties. In the next section, we investigate the electro-optical properties of a liquid crystal layer with a special Freédericksz alignment.

3. RAY-OPTICS ANALYSIS OF A LIQUID CRYSTAL-BASED ELECTRO-OPTICAL SWITCH

In this section, we present simulations of a liquid crystal-based electro-optical device that enables a switching effect due to a back reflection phenomenon.[2]

Liquid crystal can be controlled by external electric (or magnetic) fields. Interactions between boundaries and liquid crystal also have a large controlling effect. Often, the influence of the boundaries opposes the response to an electric field. The result is a threshold phenomenon called the Freédericksz transition.[9] Fig. 1-(a) shows a Freédericksz alignment of a liquid crystal layer in which the local optical axis (indicated by the director $\hat{\mathbf{d}}$) is rotated towards the direction of an external electric field. In this section, we investigate Freédericksz alignments that show bend and splay deformations and no twist deformations of liquid crystal.

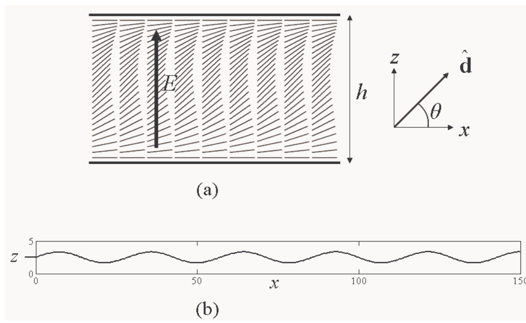

Figure 1. (a) Freédericksz alignment of a liquid crystal layer applied between two parallel glass plates, separated by a distance h. The director is rotated by an angle θ towards the direction of the electric field E. (b) Ray path of an extraordinary ray for $V_r = 1.1803$. Apparently, the optical system shows a light guiding behavior.

In Fig. 1-(a), the director $\hat{\mathbf{d}}$ lies in the xz-plane. It is convenient to write the director vector components as $\hat{d}_x = \cos[\theta(x,z)]$ and $\hat{d}_z = \sin[\theta(x,z)]$, where $\theta(x,z)$ is the angle between $\hat{\mathbf{d}}$ and the x-axis. From the symmetry of the system we can define θ_{max} as the maximum value of θ at $z = \frac{h}{2}$. Then, the potential difference V across the liquid crystal layer that corresponds to θ_{max} is given by[9]

$$V = 2\mathcal{K}(m)\sqrt{\frac{K_{11}}{\varepsilon_0 \Delta\varepsilon}}, \tag{16}$$

where $\mathcal{K}(m)$ is the complete elliptic integral of the first kind with elliptic modulus $m = \sin^2\theta_{max}$. Furthermore, $\triangle\varepsilon$ is the anisotropy in the static dielectric permittivity of the liquid crystal. K_{11} is an elastic constant with which the associated splay deformation energies scale. The threshold voltage below which the liquid crystal remains undistorted satisfies

$$V_{th} = \pi\sqrt{\frac{K_{11}}{\varepsilon_0 \Delta\varepsilon}}. \tag{17}$$

Finally, it is important to realize that the liquid crystal profile only depends on the dimensionless coordinate $\frac{z}{h}$.[9]

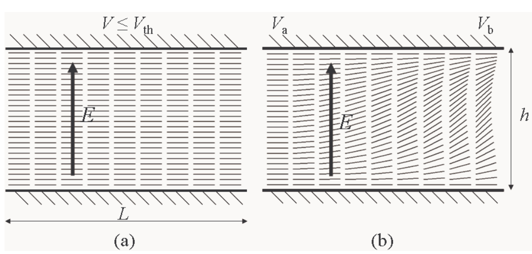

Figure 2. Liquid crystal layer applied between two ideal parallel mirrors, separated by a distance h. In (a), $V(x) \leq V_{th}$ and $\hat{\mathbf{d}} = (1,0)$. In (b), $V(x) = V_{th} + \frac{x}{L}(V_b - V_{th})$, where $L = 150$ is the total length of the optical system and $V_b > V_a$.

We consider the liquid crystal layer of Fig. 1-(a). We assume that the thickness h is at least in the order of 20 wavelengths or more. Then the properties of the liquid crystal change slowly over the distance of a wavelength and the use of the Hamiltonian method is justified. An incident light ray is linearly polarized in the xz-plane (TM mode) and propagates in the positive x-direction. At $(x, z) = (0, \frac{h}{2})$ the light ray is injected in the liquid crystal layer. Hence, the resulting light ray in the liquid crystal layer is extraordinary and then the Hamilton equations given by Eqs. 6-9 can be applied. In addition, we simulate a nematic liquid crystal with $n_o = 1.5266$ and $n_e = 1.8181$ (Merck BL009 mixture). We estimate $K_{11} = 10$ pN and $\Delta\varepsilon = 10$, yielding $V_{th} = 1.0558$ V. We define $h = 5$ and the ray path is calculated with the first-order Runge-Kutta method with step size $\Delta\tau = 0.001$. Fig. 1-(b) shows the result for the extraordinary ray path with $V_r = \frac{V}{V_{th}} = \frac{2}{\pi}\mathcal{K}(m) = 1.1803$.

From Fig. 1-(b) we can conclude that the ray path is oscillatory: the optical system shows a light-guiding behavior. The oscillatory period corresponds to a potential difference of $V = 1.2461$ V and $\theta_{max} = \frac{\pi}{4}$ radians. The light ray is modulated in the vertical z-direction, but not in the horizontal x-direction due to the absence of a gradient in the x-direction in the director profile. We can expect that a light ray is modulated both in the vertical and horizontal direction if we induce an additional horizontal gradient. In what follows below, we will show that these expectations are confirmed by our simulations.

Now let us consider a liquid crystal layer applied between two parallel ideal mirrors (100% reflectance). Similar to the configuration in Fig. 1, the corresponding director profile $\hat{\mathbf{d}}(x, z)$ is a Freédericksz alignment. This time, however, we apply a horizontal gradient in the potential difference $V = V(x)$ across the liquid crystal layer. This can be achieved with e.g. the application of a resistive electrode structure. As a result, the director profile has an additional gradient in the horizontal direction. In Fig. 2, the proposed optical design is depicted in two different situations. Fig. 2-(a) shows the situation where $V(x) \leq V_{th}$ and $\hat{\mathbf{d}}(x, z) = (1, 0)$. Hence, the properties of the liquid crystal layer are homogeneous. On the other hand, in Fig. 2-(b) we show the director profile for which $V(x) = V_{th} + \frac{x}{L}(V_b - V_{th})$, where $L = 150$ is the total length of the optical system, $V_a = V_{th} = 1.0558$ V and $V_b = 1.2461$ V, corresponding to $\theta_{max} = \frac{\pi}{4}$ radians. In this case, the director profile has a gradient both in the vertical and the horizontal direction.

First, we will investigate the situation in Fig. 2-(a), where, at $x = 0$, an incident extraordinary ray enters the liquid crystal at approximately 12° with the vertical z-direction. This extraordinary ray is repeatedly reflected by the two ideal parallel mirrors and propagates in the positive x-direction. Since the director profile $\hat{\mathbf{d}}(x, z) = (1, 0)$, the ray path of the light ray consists of straight lines. Fig. 3-(a) shows the ray path of the extraordinary light ray inside the liquid crystal. Fig. 3-(b) shows the angle of reflection φ inside the optical system as a function of the number of reflections. As expected, φ is constant throughout the system. After approximately 145 reflections, the light ray leaves the system at $x = 150$.

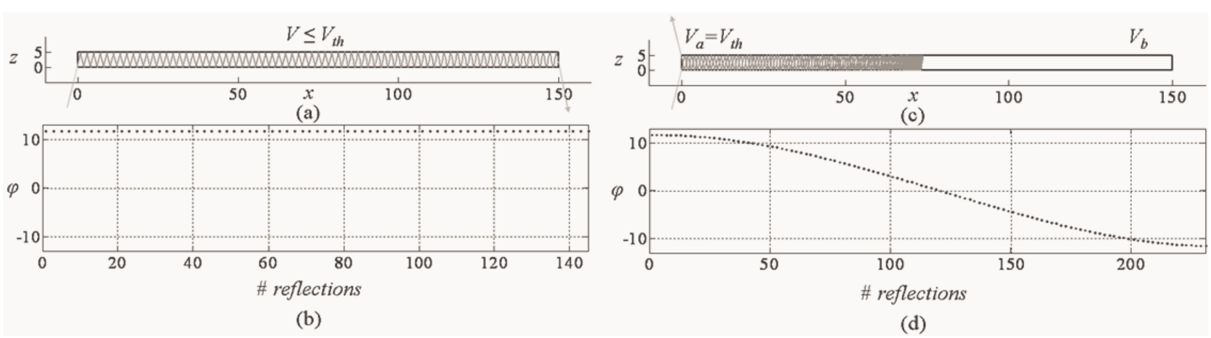

Figure 3. In (a), the ray path of the extraordinary light ray (TM mode) is depicted inside the liquid crystal layer as defined in Fig. 2-(a). In (b), the corresponding angle of reflection φ of the ray path is constant and eventually, the ray leaves the system at $x = 150$. In (c), the ray path of the extraordinary light ray is depicted inside the liquid crystal layer as defined in Fig. 2-(b). From (d), we conclude that this time the angle of reflection φ decreases along the ray path: the direction of propagation is reversed and the light ray leaves the system at $x = 0$.

Secondly, we examine the configuration of Fig. 2-(b), where the light ray enters the liquid crystal again at $x = 0$ at 12°. The light ray is reflected by the two ideal parallel mirrors and initially propagates in the positive

x-direction. Since in this case the director profile $\hat{\mathbf{d}}(x, z)$ is inhomogeneous, the ray path of the light ray is curved and affected in the horizontal direction. Due to the presence of a lateral gradient in the liquid crystal profile and the well-known fact that light bends towards regions with high refractive index, φ decreases after each reflection, see Fig. 3-(d). After 120 reflections ($x \approx 75$), φ is reduced to negative values. These negative values for φ imply that the ray is now propagating in the negative x-direction. After 240 reflections, the light ray leaves the system at $x = 0$, as can be seen in Fig. 3-(c). From these observations, we can conclude that the horizontal direction of propagation of the ray is back reflected due to the lateral gradient in the director profile.

We have shown that a two-dimensional gradient in a liquid crystal layer with a Freédericksz alignment applied between two ideal parallel mirrors enables a back reflection phenomenon in which the direction of propagation of extraordinary light rays (TM mode) is reversed. As a result, the propagation direction of light in the proposed optical system can be switched by means of an external electric field. Hence, the optical system behaves like an electro-optical switch. In earlier publication, we suggest a number of measures to optimize the efficiency of the electro-optical switch.[2] There we conclude that a total efficiency of 10% or higher is feasible. In addition, we point out the self confinement of spatial optical solitons in nematic liquid crystal cells: in Beeckman[10] simulations reveal an oscillatory self-confined light beam in a 75 μm thick liquid crystal cell, similar to the optical behavior presented in Fig. 1-(b).

4. RAY-OPTICS ANALYSIS OF A LIQUID CRYSTAL-BASED LIGHT GUIDE STRUCTURE

In this section, we discuss the working principle of a liquid crystal-based light guide structure. This liquid crystal light guide structure enables a controlled extraction of TM-polarized light by selectively applying a voltage to electrode structures. In addition, we present ray-tracing results of the simulated optical properties of the liquid crystal light guide structure. These results are intended to give the reader a first impression of the optical behavior and potential use of the device discussed. In particular, our goal is to show that the Hamiltonian method provides us with a tool to obtain a first impression of the optical behavior of such a complex optical system.

4.1 Device Principle

A schematic cross section of the device is depicted in Fig. 4 (xz-plane). The device consists of two parallel glass plates with a liquid crystal layer in between. The bottom glass plate is equipped with a pattern of transparent conducting ITO (Indium Tin Oxide) line electrodes with their long axis perpendicular to the plane of the figure (y-direction). The glass plates are covered with alignment layers that orient the liquid crystal in the y-direction, i.e. when there is no voltage applied to the electrodes. Then the optical properties of the liquid crystal profile are homogeneous and the local optical axis of the liquid crystal, indicated by the unit vector $\hat{\mathbf{d}}(x, y, z)$ (the director), is given by $\hat{\mathbf{d}} = (0, \pm 1, 0)$. From the left the liquid crystal device is illuminated by an unpolarized light source. There, light is injected into the liquid crystal layer and the glass plates. Due to total internal reflection at the top and bottom glass-air interfaces, the injected light is trapped and guided in the positive x-direction. In conclusion, when no voltage is applied to the electrodes, the liquid crystal device behaves like a light guide.

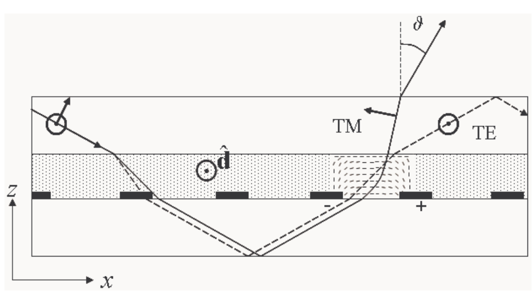

Figure 4. Working principle of the liquid crystal light guide structure. When a voltage is locally applied to the electrodes, the director $\hat{\mathbf{d}}$ aligns along the electric field lines. TM-polarized light is affected by the resulting local gradients in the liquid crystal and is extracted from the device. TE-polarized light remains inside the device due to a light guiding effect.

When a low voltage is applied to the electrodes, the liquid crystal aligns along the electric field lines and the director lies in the xz-plane (see Fig. 4). Then, the optical properties of the liquid crystal profile are inhomogeneous, i.e. the director $\hat{\mathbf{d}}$ depends on the position inside the liquid crystal layer. As a result, the index of refraction not only varies with direction but also with position. Therefore the light paths of light rays inside the liquid crystal are curved. This is due to the fact that light bends towards regions with high refractive index. However, the two-dimensional gradient in the liquid crystal only affects light with a linear polarization in the xz-plane (TM polarization): only extraordinary light rays are curved. Extraordinary light rays are deflected from the linear trajectory in the liquid crystal layer and can be extracted from the top and bottom glass plates of the device. Ordinary light rays with a linear polarization in the y-direction (TE polarization) are not affected by the gradients in the optical properties. Hence the corresponding light paths are always straight lines. Similar to the case in which $\hat{\mathbf{d}} = (0, \pm 1, 0)$ (homogeneous alignment), ordinary light rays are trapped and guided by the liquid crystal device.

For the type of application we are interested in, the light guiding of ordinary rays is not a desired effect when a voltage is applied to the electrodes. This problem can be overcome if the ordinary rays are somehow recycled and transformed into polarization sensitive light. This can be achieved by using, for example, depolarizing diffusing reflectors at one or more sides of the liquid crystal device. However, for simplicity, we do not take this scenario into account and focus our attention to the optical response of extraordinary light rays.

Summarizing, the liquid crystal light guide structure enables a controlled extraction of TM-polarized light by selectively applying a voltage to the electrode structures. As a result, the device enables local dimming and highlighting, a feature that is desired for applications such as polarized backlight architectures.[?]

4.2 Modeling Aspects of the Light Guide Structure

In order to model the optical properties of the liquid crystal-based light guide structure, we apply the Hamilton equations for extraordinary rays. Before the Hamilton equations can be applied, the director profile $\hat{\mathbf{d}}$ of the liquid crystal needs to be calculated. Numerical director profiles are produced by optical analysis software programs, like LCD Master[11] or 2dimMOS.[12] We calculated the liquid crystal profile obtained for one period of the electrode structure. This period is defined as the liquid crystal profile induced by two electrodes: one electrode with a positive voltage and one with a negative voltage. Fig. 5 shows a typical numerical director profile calculated by 2dimMOS. The dimensions of the simulated liquid crystal region are also indicated. The period and height are indicated by T and H, respectively. The width of the electrodes and the inter-electrode distance correspond to w and t, respectively. The periodical director profile is repeated in the horizontal direction, hence producing a liquid crystal cell as depicted in Fig. 4.

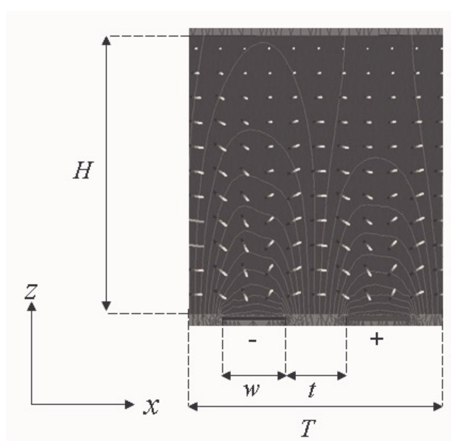

Figure 5. Typical result of a director profile calculated by 2dimMOS. The director is indicated by the bars and the contour lines represent the equipotential lines. The director at the top is aligned in the y-direction, whereas the director is in the xz-plane at the bottom of the liquid crystal cell. The period and height of the liquid crystal region are indicated by T and H, respectively. The width of the electrodes and the inter-electrode distance are indicated by w and t, respectively. In this particular case, $T = 12\mu$m, $H = 6.4\mu$m, $w = 3\mu$m and $t = 3\mu$m.

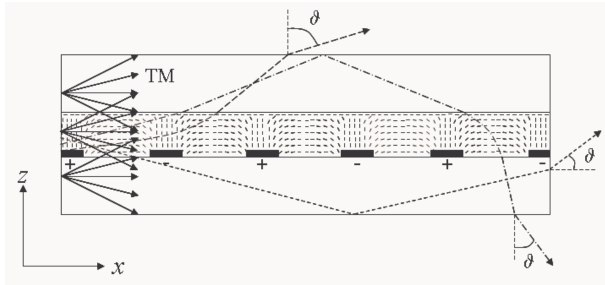

Figure 6. The illumination is simulated by the injection of TM-polarized light rays into the left side. The light rays exit the liquid crystal cell through the top, bottom and right side of the device. The angle of refraction is indicated by the angle ϑ.

To simplify the modeling aspects, we assume that the electric field is strong enough to induce a twist of 90° in the xy-plane: the director lies in the xz-plane. The assumption that the director lies in the plane of the drawing is in good agreement with the numerical results depicted in Fig 5. The upper region of the director profile clearly shows a twist and there the director has a component perpendicular to the plane of the drawing. However, the gradients of the director in this region of the liquid crystal layer are not expected to affect the ray paths of light rays significantly. Therefore, in a good approximation, the director can be assumed in the plane of the drawing: $\hat{d}_y = 0$. For the moment, a two-dimensional approach is sufficient in order to obtain a good understanding of the optical properties.

The illumination of the light guide structure is simulated by the injection of light rays with initial positions and directions of propagation along the vertical edge (see Fig. 6). We define a discrete set of initial values for the position and direction, as can be seen in Fig. 6. In order to simulate the optical properties of the device we trace a sufficient number of TM-polarized rays through the glass and liquid crystal layer when a voltage is applied to the electrodes. In the ray-tracing simulations, we also include the possibility that rays can be totally reflected at the top and bottom glass-air interfaces (total internal reflection). When this is the case, the ray tracing continues until the rays finally enter the exterior of the device. In particular, we calculate the angle ϑ under which the light is transmitted at the top and bottom glass-air interfaces of the liquid crystal device (see Fig. 6). In addition, we also calculate the light output from the side at the right. The number of transmitted rays obtained for a certain angular range is a measure for the light intensity. In this way, we obtain angular intensity distributions for the top, bottom and right side of the device.

4.3 Ray-Tracing Results

In order to obtain a first impression of the optical behavior, we calculate the ray paths of a number of rays when a voltage is applied to the electrode structure. In the ray-tracing simulations we define an un-collimated light source that illuminates the light guide structure from the left. This light source is modeled by injecting (TM-polarized) light rays into the device at certain angles and positions. For each initial position $\mathbf{r}(\tau_0)$ five rays are defined with an angle of incidence with respect to the horizontal axis at 60°, 30°, 0°, −30° and −60° (see also Fig. 6). The initial positions of the rays (and the corresponding vectors $\mathbf{p}_e(\tau_0)$) are distributed along the vertical rim of the device at 300 equidistant positions. The total amount of rays injected into the glass and the liquid crystal is therefore 1500.

The position $\mathbf{r}(\tau)$ and the vector $\mathbf{p}_e(\tau)$ of the rays inside the liquid crystal are calculated with the first-order Runge-Kutta method.[8] For an arbitrary interval $[\tau_N, \tau_N + \Delta\tau]$, with $N \in \mathbb{N}$, the x- and z-components of the position and extraordinary phase velocity vector are given by

$$x(\tau_N + \Delta\tau) = x(\tau_N) + \triangle\tau \frac{\partial \mathcal{H}_e}{\partial p_{ex}}(\tau_N), \tag{18}$$

$$z(\tau_N + \Delta\tau) = z(\tau_N) + \triangle\tau \frac{\partial \mathcal{H}_e}{\partial p_{ez}}(\tau_N), \tag{19}$$

$$p_{ex}(\tau_N + \Delta\tau) = p_{ex}(\tau_N) - \triangle\tau \frac{\partial \mathcal{H}_e}{\partial x}(\tau_N), \tag{20}$$

$$p_{ez}(\tau_N + \Delta\tau) \quad = \quad p_{ez}(\tau_N) - \triangle\tau \frac{\partial \mathcal{H}_e}{\partial z}(\tau_N), \tag{21}$$

with the partial derivatives of $\mathcal{H}_e$ given by Eqs. 8 and 9. The step size $\triangle\tau$ that is used in the simulations is 0.05.

The properties of the liquid crystal layer that we use in the simulations are listed in Table 1. There, the elastic constants with which the elastic splay, twist and bend deformation energies scale are given by K_{11}, K_{22} and K_{33}, respectively. The static dielectric permittivity of the liquid crystal is given by $\triangle\varepsilon = \varepsilon_{||} - \varepsilon_{\perp}$ and the viscosity of the liquid crystal is defined γ. The values listed in Table 1 correspond to a realistic type of liquid crystal (BL009 mixture).

Table 1. Liquid crystal properties utilized in the simulations.

parameter	value
n_o	1.5266
n_e	1.8181
K_{11} (pN)	17.9
K_{22} (pN)	7.0
K_{33} (pN)	33.5
$\Delta\varepsilon$	15.5
γ (cSt)	83

The thickness of the glass substrates is defined to be only 2 μm. This order of magnitude is not realistic for the thickness of a glass substrate. However, in the first approximations that we use, this is of little importance for the simulations since, for the moment, we are mainly interested in the angular optical response of the device and not so much in the position-dependent optical properties.

The numerical director profile $\hat{\mathbf{d}}$ calculated by 2dimMOS is given on the grid points of a regular two-dimensional grid (see Fig. 5). In the simulations, the grid represents a matrix of 7993 columns, corresponding to a length of 28 μm, and 321 rows, corresponding to a height H of 6.4 μm. The width w of the electrodes and inter-electrode distance t on the bottom glass substrate are both defined to be 4 μm. The voltage applied to the electrodes is 5 V. The spatial resolution of the grid is limited and for an accurate calculation of the ray path inside the liquid crystal, it is necessary to apply interpolation techniques in order to obtain the director in intermediate space. Note that the order for the interpolation of the director profile in intermediate space must be the order of the Runge-Kutta method.

As mentioned before, we calculate the angular intensity distribution of the top, bottom and right side of the light guide structure. The angular intensity distribution I for the top side is depicted in Fig. 7-(a). The results are presented by a histogram: each angular interval $\triangle\vartheta = 1°$ corresponds to a number of collected rays. From these results we can conclude that the majority of the light that is transmitted at the top side propagates at angles larger than 60°. The remaining light is transmitted towards lower angles. Moreover, for some light rays the angle ϑ is even negative. A negative value for ϑ means that light rays are propagating in the negative x-direction. Although physically possible, these kind of light rays rarely occur in the ray-tracing simulations.

The angular intensity distribution for the bottom side is depicted in Fig. 7-(b). The light transmitted from the bottom glass substrate is primarily propagating between $-10°$ and $-60°$. The negative values for the angle ϑ correspond to a direction of propagation in the positive x-direction. Apparently, the angular intensity distributions of the top and bottom side do not resemble each other. Hence, we can conclude that, according to the ray-tracing simulations, the optical response of the liquid crystal light guide structure is different for the top and bottom sides. In particular, the intensity profile of the top side is confined in a smaller angular range than the intensity profile for the bottom side.

Only an insignificant part of the (TM-polarized) light is guided by the liquid crystal device and transmitted through the right side. Almost all of the incident light is transmitted through the top and bottom glass substrates. Therefore, the simulations support the idea of a controlled extraction of light when a voltage is applied to the electrode structure.

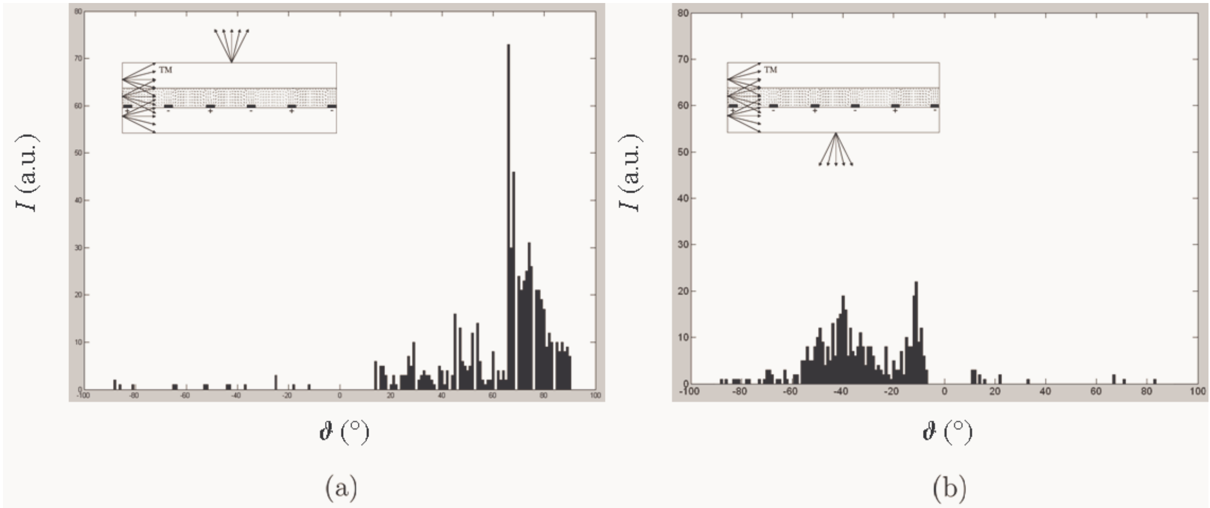

Figure 7. (a) Angular intensity distribution I for the top side of the liquid crystal light guide structure. The histogram shows the number of collected rays for each angular interval $\Delta\vartheta = 1^\circ$. Most of the light rays are collected in the range between approximately 65° and 80°. (b) Angular intensity distribution I for the bottom side of the liquid crystal beam control device. The negative values for ϑ correspond to rays propagating in the positive x-direction.

In general, we can conclude that the preliminary ray-tracing simulations support the working principle of the liquid crystal light guide structure. Moreover, the optical response at the top side shows an angular intensity distribution that is confined in a relatively narrow angular range. This angular range lies approximately between 65° and 80°.

4.4 Comparison with Experimental Results

To verify some of the simulation results, we measured the angular intensity distribution emerging from the top glass substrate of a liquid crystal cell. We characterized a liquid crystal cell with design parameters resembling the configuration used inn our simulations: the thickness H of the liquid crystal layer (see Table 1) is 5 μm and the width of the electrodes and the inter-electrode distance is 4 μm. The voltage applied to the electrodes is 5 V.

The liquid crystal cell was placed in a side-lit configuration directly in contact with a cold-cathode fluorescence lamp (CCFL). The angular luminance was measured with an EZContrast 160 conoscope from Eldim S.A..[13] Fig. 8-(a) shows a typical result of such an analysis. These results clearly resemble the angular characteristics obtained by the ray-tracing simulations (see Fig. 7-(a)): the light is typically confined in the angular range for ϑ approximately above 60°. The plane which corresponds to the xz-plane in the model ($y = 0$) is indicated in Fig. 8-(a) by the arrow. The angular intensity distribution measured in this plane can be compared with the two-dimensional simulations of Fig. 7-(a). For an accurate comparison between simulations and experiment, the measured luminance (cd/m^2) is scaled by a factor $\cos(\vartheta)$ to obtain the relative luminance intensity (cd).

Fig. 8-(b) shows the simulated intensity distribution (histogram) depicted in Fig. 7-(a) together with the experimental intensity distribution for $y = 0$. We can see that the theoretical results and the experimental results are in a fair agreement: the high intensity region between approximately 65° and 80° is confirmed by the experimental results. The rapid decrease in the measured angular intensity at 80° is explained by the limited angular range of the conoscope that lies between -80° and 80°.

On the other hand, the results do not match quantitatively. The correspondence between model and experiment is limited by, for example, the computational power of the ray-tracing simulation program, i.e. the number of rays. Another reason for a mismatch between theory and experiment can be due to the fact that near the electrode structures of the light guide the material properties of the liquid crystal can change rapidly with respect to the wavelength of light. On the other hand, the Hamiltonian method is based on the assumption that the properties of a medium change slowly over the distance of a wavelength. This means that in some regions in

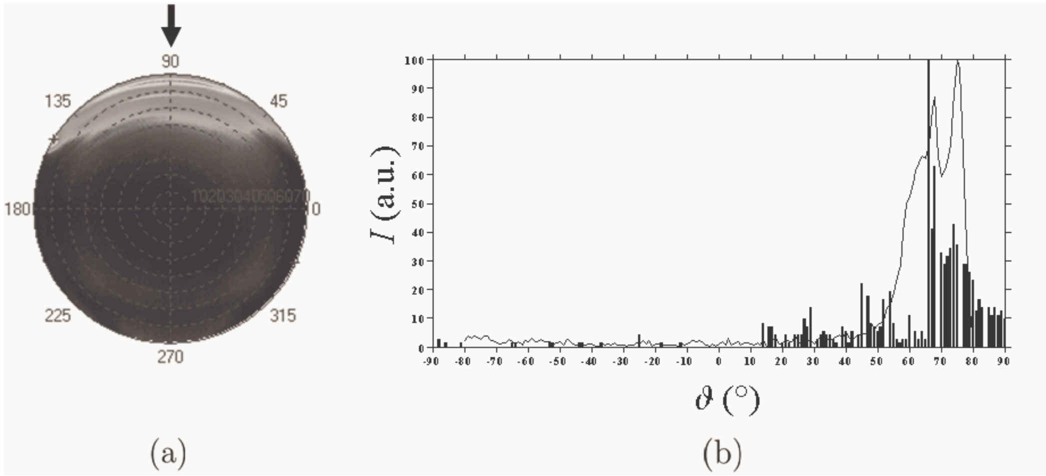

Figure 8. (a) Polar coordinate plot of a typical light profile measured by the EZContrast 160 conoscope. Note that the transmitted light is confined in the angular range for ϑ approximately above 60°. The plane which corresponds to the plane $y = 0$ in the model and the simulations is indicated by the arrow. (b) The experimental results (curve) and the numerical results (histogram) for the top side depicted in one diagram. The angular region where the simulated light intensity is maximal lies approximately between 65° and 80°. This observation is confirmed by the experimental results.

the liquid crystal the Hamiltonian method can give rise to unrealistic light paths. As a consequence, not all ray paths calculated in the simulations necessarily represent physical light rays and some ray paths might deviate from the actual ray path inside the liquid crystal. In addition to this, yet another explanation for the discrepancy can be ascribed to the fact that the ray-tracing simulations are performed in two dimensions, whereas the experiment has a three-dimensional character, including diffraction effects. In addition, light can be scattered by the pollution of the glass surfaces and absorbed by the transparent conducting ITO electrode structures. Because of these imperfections, the ray-tracing results presented in this section should be considered as a first approximation of the actual optical properties of the liquid crystal-based light guide structure.

5. CONCLUSIONS AND DISCUSSION

We have shown that the Hamiltonian method enables the modeling of the optical properties in the geometrical-optics approach of in general inhomogeneous uniaxially anisotropic media. This statement is true provided that the optical properties of a medium change slowly over the distance of a wavelength. In particular, we have investigated the optical properties of two inhomogeneous liquid crystal-based optical configurations.

In a first example, we have shown that a two-dimensional gradient in a liquid crystal layer with a Freédericksz alignment applied between two parallel mirrors enables a back reflection phenomenon in which the direction of propagation of extraordinary light rays (TM mode) is reversed. The propagation direction of light in the optical system discussed can be switched by means of an external electric field. As a result, the optical system behaves like an electro-optical switch. For this optical configuration, the use of the Hamiltonian method is justified since we have assumed an inhomogeneous liquid crystal layer with a thickness of at least 20 wavelengths.

In a second example, we have simulated the optical properties of a liquid crystal-based light guide structure which enables a controlled extraction of TM-polarized light when a voltage is applied to electrode structures. From ray-tracing simulations we can conclude that the numerical results obtained form the Hamiltonian method support the working principle of the liquid crystal device. The ray-tracing simulations show that the angular intensity distribution for the top side is confined in a relatively narrow angular range. This angular range lies approximately between 65° and 80°. Qualitatively, this result is in good agreement with experimental results. However, the correspondence between model and experiment is limited by the computational power of the ray-tracing simulation program, i.e. the number of rays. In addition, the liquid crystal contains regions where the material properties change rapidly over the distance of a wavelength, which is in contradiction with the rules of geometrical optics. As a consequence, not all ray paths calculated in the simulations necessarily represent physical light rays and some ray paths might deviate from the actual ray path inside the liquid crystal. Finally, the ray-tracing simulations are performed in two dimensions, whereas the experiment has a three-dimensional character, including diffraction effects, absorption and scattering of the light. Because of these imperfections, the ray-tracing results presented for the liquid crystal-based light guide structure should be considered a first approximation of the actual optical properties.

It has been shown that, given an arbitrary director profile, our polarized ray-tracing method can be applied to calculate curved ray paths of light rays in inhomogeneous anisotropic media. When the method is implemented in a ray-tracing simulation program, we are able to assess the optical properties of complex anisotropic optical systems.

ACKNOWLEDGMENTS

We would like to thank Romain Esteve for a fruitful cooperation and his valuable contributions to this work. Also, we would like to thank Hugo Cornelissen and Thomas Kraan for fruitful discussions.

REFERENCES

[1] M. Sluijter, D. K. G. de Boer and J. J. M. Braat, “General polarized ray-tracing method for inhomogeneous uniaxially anisotropic media,” *J. Opt. Soc. Am. A* **25**, pp. 1260–1273, 2008.

[2] M. Sluijter, D. K. G. de Boer and H. P. Urbach, “Simulations of a liquid crystal-based electro-optical switch,” accepted for publication in Optics Letters (Vol. 34, No. 2).

[3] J. Strömer, G. Cennini, M. Sluijter and D. K. G. de Boer, “A novel light guide structure capable of local light outcoupling,” to be published.

[4] H. J. B. Jagt, H. J. Cornelissen, D. J. Broer, C. M. W. Bastiaansen, “Linearly polarized light emitting backlight,” *J. SID* **10**, pp. 107–112, 2002.

[5] H. J. Cornelissen, H. P. M. Huck, D. J. Broer, S. J. Picken, C. M. W. Bastiaansen, E. Erdhuizen, N. Maaskant, “Polarized light LCD backlight based on liquid crystalline polymer film: a new manufacturing proces,” *SID 04 Digest*, pp. 1178–1181, 2004.

[6] M. Kline and I. W. Kay, *Electromagnetic theory and geometrical optics*, pp. 110–117, John Wiley & Sons, New York, 1965.

[7] M. Sluijter, D. K. G. de Boer and H. P. Urbach, “Ray-optics analysis of inhomogeneous biaxially anisotropic media,” accepted for publication in J. Opt. Soc. Am. A.

[8] W. Press, S. A. Teukolsky, W. T. Vetterling and B. P. Flannery, *Numerical recipes in FORTRAN, The art of Scientific Computing*, pp. 704–708, Cambridge University Press, Cambridge, 1992.

[9] P. J. Collings and M. Hird, *Introduction to liquid crystals, Chemistry and Physcis*, pp. 202–210, Taylor & Francis, London, 1997.

[10] J. Beeckman, K. Neyts, X. Hutsebaut, C. Cambournac and M. Haelterman, “Simulation of 2D lateral light propagation in nematic liquid crystal cells with tilted molecules and nonlinear reorientational effect,” *Opt. Quant. Electron.* **37**, pp. 95–106, 2005.

[11] SHINTECH.Inc, http://www.shintech.jp.

[12] AUTRONIC MELCHERS GmbH, http://www.autronic-melchers.com.

[13] ELDIM manufacturer of 2D photometers & colorimeters and inspection systems, www.eldim.fr.